INTECH
open science | open minds

OPEN ACCESS
ARTICLE

International Journal of Advanced Robotic Systems

Square Root - Type Control for Robot Manipulators

Regular Paper

Fernando Reyes[1], Jaime Cid[2,*], Miguel Angel Limon[1] and Manuel Cervantes[3]

1 Facultad de Ciencias de la Electrónica BUAP, Mexico
2 Vicerrectoría de Investigación y Estudios de PosgradoCUVyTT-BUAP, Mexico
3 Departamento de Mecatronica UPAEP, Mexico
* Corresponding author E-mail: jcid@ece.buap.mx

Received 30 May 2012; Accepted 20 Aug 2012

DOI: 10.5772/52500

Abstract This paper addresses the problem of position control for robot manipulators. A new control structure with compensation for global position is presented. The main contribution of this paper is to prove that the closed loop system of the nonlinear robot dynamics model and the proposed control algorithm is globally, asymptotically stable and in agreement with Lyapunov's direct method and LaSalle's invariance principle. Besides this, the theoretical results in a real-time experimental comparison are also presented to show a comparison of the performance between the square root type controller and simple PD scheme on a three degrees-of-freedom direct-drive robot.

Keywords Robot, Direct driver, Stability, PD control

1. Introduction

Industrial robots are basically positioning and handling devices. A useful robot is one that is able to carry outa programmed task. The control of robot manipulators requires knowledge of the dynamics model and its mathematical properties. The problem of position control (also called regulation) is one the most relevant issues in robotics - this is especially so in the case of motion control or trajectory control. The main goal of position control in a joint space is to move the manipulator end-effector to a fixed desired target, which is assumed to be constant regardless of its joint position. In position control, the simple PD scheme was the most widely used algorithm studied in Takegaki and Arimoto [1]; meanwhile, Arimoto and Miyazaki [2] yield a global asymptotically stable closed-loop system for a trivial selection of proportional and derivative gains [2]. By way of contrast, the simple PID control is another popular strategy. However, it lacks a global asymptotic stability proof [3-5].

In recent years, various PD-type control schemes have been developed for the position control of robot manipulators. Among them, the following can be cited: a class of PID and PD controllers for position in [3-5]; a PD controller with proportional and derivative gains as nonlinear functions of the robot's states proposed in [6]; the methodology of energy shaping to propose many global regulation schemes in [7-8]; energy functions based on Lyapunov's stability theory to design control schemes in [9-13]; a sliding PID control for robot manipulators in [14]; a control algorithm with fuzzy logic in [15]; and a methodology on a$\mathcal{L}_1$ adaptive controller as presented in [16].

In view of the simplicity and applicability of the simple PD control in industrial applications, the main motivation of this paper is to propose both theoretical development and practical applications with high performance.

The objective of this work is to present a new control scheme that leads to global asymptotic stability in agreement with Lyapunov's direct method and Lasalle's invariance principle of the closed-loop system as formed by the nonlinear dynamics model of a n degrees-of-freedom robot manipulator and the control structure. The new family has a nonlinear structure, which incorporates square-root type-components to quickly drive the position error to equilibrium point. The proposed control falls into the category of joint-level control and it requires that the set-point or desired position will be given at the joint space.

This paper also presents real-time experiments for position control on a three degrees-of-freedom direct-drive robot manipulator. The experimental results consist of a comparison of the performance between the proposed control and a popular PD scheme using the $\mathcal{L}_2$ norm.

This paper is organized as follows. Section 2 recalls the robot dynamics and useful properties for stability analysis. In Section 3, the proposed algorithms for the control and analysis of global asymptotic stability are presented. Section 4 describes the experimental setup based on the three degrees-of-freedom direct-drive robot manipulator and the experimental comparison between the proposed scheme and PD control. Section 5 contains the experimental comparison between PD and square root-type controllers. Finally, some conclusions are offered in Section 6.

2. Robot dynamics

The dynamics of a serial n-link rigid robot manipulator with viscous friction can be written as [17-18]:

$$\boldsymbol{\tau} = M(\boldsymbol{q})\ddot{\boldsymbol{q}} + C(\boldsymbol{q},\dot{\boldsymbol{q}})\dot{\boldsymbol{q}} + B\,\dot{\boldsymbol{q}} + \boldsymbol{g}(\boldsymbol{q}) \tag{1}$$

where $\boldsymbol{q}$is then$\times$ 1vector of joint displacements,$\dot{\boldsymbol{q}}$is then$\times$ 1 vector of joint velocities, $\ddot{\boldsymbol{q}}$is then$\times$ 1 vector of joint acceleration,$\boldsymbol{\tau}$is then$\times$ 1 vector of input torques, $M(\boldsymbol{q})\epsilon\,\mathbb{R}^{n\times n}$ represents thesymmetric positivedefinite inertia matrix, $C(\boldsymbol{q},\dot{\boldsymbol{q}})\epsilon\,\mathbb{R}^{n\times n}$is the matrix of centripetal and Coriolis torque, $\boldsymbol{g}(\boldsymbol{q})\epsilon\,\mathbb{R}^{n\times 1}$ is the vectorof gravitational torquesobtained asthe gradient of the robot's potential energy due to gravity and$B\,\epsilon\,\mathbb{R}^{n\times n}$is the matrixof viscous friction coefficients. The vector of friction torques is assumed to be dissipative energy at all nonzero velocities and, therefore, their entries are bounded within the first and third quadrants. For zero velocities, only static friction is present.

It is assumed that the robot links are joined together with revolute joints. Although the dynamics model (1) is complex, it has several fundamental properties which can be exploited to facilitate control system design. In particular, the following are useful.

Property 1:the matrix$C(\boldsymbol{q},\dot{\boldsymbol{q}})$and the time derivate of the inertia matrix$\dot{M}(\boldsymbol{q})$ satisfy [17-18]:

$$\dot{\boldsymbol{q}}\left[\tfrac{1}{2}\dot{M}(\boldsymbol{q}) - C(\boldsymbol{q},\dot{\boldsymbol{q}})\right]\dot{\boldsymbol{q}}^T = 0, \forall\, \boldsymbol{q},\dot{\boldsymbol{q}}\ \in\ \mathbb{R}^{\boldsymbol{n}}. \tag{2}$$

This property is called skew symmetry and implies that the robot dynamics define a passive mapping between joint torque and joint velocity.

Property 2: the time derivative of the inertia matrix $\dot{M}(\boldsymbol{q})$ satisfies [17-18]:

$$\dot{M}(\boldsymbol{q}) = C(\boldsymbol{q},\dot{\boldsymbol{q}}) + C(\boldsymbol{q},\dot{\boldsymbol{q}})^T. \tag{3}$$

Property 3: the matrix$C(\boldsymbol{q},\dot{\boldsymbol{q}})$ satisfies:

$C(\boldsymbol{q},\dot{\boldsymbol{q}}) = 0\,\epsilon\,\mathbb{R}^{n\times n}$, if thejoint velocity vector is zero,$\dot{\boldsymbol{q}} = 0$[17-18].

3. Square root-type controller

In this section, we present the stability analysis of the equilibrium point for the closed-loop system formed by a nonlinear robot dynamics model and the proposed control scheme. The main feature of this new algorithm is that global asymptotic stability is guaranteed with torques inside the prescribed bounds and the response is smooth without oscillations.

Consider the following control scheme with gravity compensation given by:

$$\boldsymbol{\tau} = K_p\frac{\tilde{\boldsymbol{q}}}{\sqrt{\tilde{\boldsymbol{q}}^2+1}} - K_v\frac{\dot{\boldsymbol{q}}}{\sqrt{\dot{\boldsymbol{q}}^2+1}} + \boldsymbol{g}(\boldsymbol{q}) \tag{4}$$

where $K_p\,\epsilon\,\mathbb{R}^{n\times n}$ istheproportionalgain, which is adiagonal matrix, $K_v\epsilon\,\mathbb{R}^{n\times n}$ isa positivedefinite matrix (also calledderivativegain),$\tilde{\boldsymbol{q}}\epsilon\,\mathbb{R}^{n\times 1}$ is the vector of position error, which is defined as $\tilde{\boldsymbol{q}} = \boldsymbol{q_d} - \boldsymbol{q}(\boldsymbol{t})$,and $\boldsymbol{q_d}\,\epsilon\,\mathbb{R}^{n\times 1}$is the desired joint position. We introduce the following notation:

$$\frac{\tilde{\boldsymbol{q}}}{\sqrt{\tilde{\boldsymbol{q}}^2+1}} = \begin{bmatrix} \frac{\tilde{q}_1}{\sqrt{\tilde{q}_1^2+1}} \\ \frac{\tilde{q}_2}{\sqrt{\tilde{q}_2^2+1}} \\ \vdots \\ \frac{\tilde{q}_n}{\sqrt{\tilde{q}_n^2+1}} \end{bmatrix} \text{ and } \frac{\dot{\boldsymbol{q}}}{\sqrt{\dot{\boldsymbol{q}}^2+1}} = \begin{bmatrix} \frac{\dot{q}_1^2}{\sqrt{\dot{q}_1^2+1}} \\ \frac{\dot{q}_2^2}{\sqrt{\dot{q}_2^2+1}} \\ \vdots \\ \frac{\dot{q}_n^2}{\sqrt{\dot{q}_n^2+1}} \end{bmatrix}. \tag{5}$$

Figure 1 shows the profile type for the proposed control structure - it is a continuous function, monotonically increasing and it is also bounded.

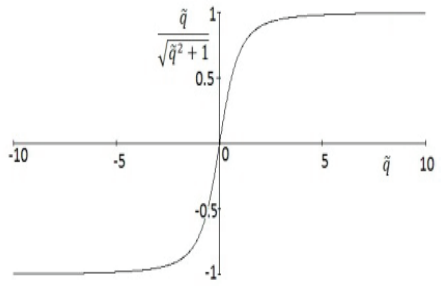

Figure 1. Saturated function for the control structure.

The control problem can be stated as to find a control law$\boldsymbol{\tau}$and select the design matricesK_p and K_v, such that the position error $\tilde{\boldsymbol{q}}(t)$and joint velocity$\dot{\boldsymbol{q}}(t)$vanish asymptotically to zero (the equilibrium point is achieved), i. e.:

$$\lim_{t\to\infty}\begin{bmatrix}\tilde{\boldsymbol{q}}(t)\\ \dot{\boldsymbol{q}}(t)\end{bmatrix} = \mathbf{0} \in \mathbb{R}^{2n} \forall\, t \geq 0.$$

Proposition: Consider the robot dynamic model (1) together with the control law (4), then the closed loop system is globally asymptotically stable and the positioning aims $\lim_{t\to\infty}\boldsymbol{q}(t) = \boldsymbol{q_d}$y and $\lim_{t\to\infty}\dot{\boldsymbol{q}}(t) = 0$ are achieved.

Proof: The closed-loop system equation obtained by combining the robot dynamics model (1) and the control structure (4) can be written as:

$$\frac{d}{dt}\begin{bmatrix}\tilde{\boldsymbol{q}}\\ \dot{\boldsymbol{q}}\end{bmatrix} = \begin{bmatrix}-\dot{\boldsymbol{q}}\\ M^{-1}(\boldsymbol{q})[K_p\frac{\tilde{q}}{\sqrt{\tilde{q}^2+1}} - K_v\frac{\dot{q}}{\sqrt{\tilde{q}^2+1}} - B\dot{\boldsymbol{q}} - C(\boldsymbol{q},\dot{\boldsymbol{q}})\dot{\boldsymbol{q}}]\end{bmatrix} \quad (6)$$

Which is an autonomous differential equation and the origin of this joint state space is its unique equilibrium point.

We propose the following Lyapunov function candidate to carry out the stability analysis of equation (6):

$$V(\tilde{\boldsymbol{q}},\dot{\boldsymbol{q}}) = \frac{1}{2}\dot{\boldsymbol{q}}^{\boldsymbol{T}} M(\boldsymbol{q})\dot{\boldsymbol{q}} + 2\begin{bmatrix}\sqrt{\sqrt{\tilde{q}_1^2+1}-1}\\ \sqrt{\sqrt{\tilde{q}_2^2+1}-1}\\ \vdots\\ \sqrt{\sqrt{\tilde{q}_n^2+1}-1}\end{bmatrix}^T K_p \begin{bmatrix}\sqrt{\sqrt{\tilde{q}_1^2+1}-1}\\ \sqrt{\sqrt{\tilde{q}_2^2+1}-1}\\ \vdots\\ \sqrt{\sqrt{\tilde{q}_n^2+1}-1}\end{bmatrix} \quad (7)$$

The first term of $V(\tilde{\boldsymbol{q}},\dot{\boldsymbol{q}})$ is a positive function with respect to the state variable $\dot{\boldsymbol{q}}$ because $M(\boldsymbol{q})$is a positive definite matrix. The second term in the Lyapunov function candidate represents the potential energy induced by the position error. Note that for each component which satisfies$\sqrt{\tilde{q}_i^2+1} \geq 1 > 0$,then it is true that $\sqrt{\tilde{q}_i^2+1} - 1 > 0, \forall\, i = 1,2,\dots,n$; this term is also a positive definite function since K_p is a diagonal definite positive matrix. Therefore, equation (4) is a globally positive definite and radially unbounded function.

The time derivative of the Lyapunov function candidate (7) along the trajectories of the closed loop equation (6) is given by:

$$\dot{V}(\tilde{\boldsymbol{q}},\dot{\boldsymbol{q}}) = \dot{\boldsymbol{q}}^{\boldsymbol{T}} M(\boldsymbol{q})\ddot{\boldsymbol{q}} + \frac{1}{2}\dot{\boldsymbol{q}}^{\boldsymbol{T}}\dot{M}(\boldsymbol{q})\dot{\boldsymbol{q}} + \frac{d}{dt}2\begin{bmatrix}\sqrt{\sqrt{\tilde{q}_1^2+1}-1}\\ \sqrt{\sqrt{\tilde{q}_2^2+1}-1}\\ \vdots\\ \sqrt{\sqrt{\tilde{q}_n^2+1}-1}\end{bmatrix}^T K_p \begin{bmatrix}\sqrt{\sqrt{\tilde{q}_1^2+1}-1}\\ \sqrt{\sqrt{\tilde{q}_2^2+1}-1}\\ \vdots\\ \sqrt{\sqrt{\tilde{q}_n^2+1}-1}\end{bmatrix} \quad (8)$$

$$\frac{d}{dt}2\begin{bmatrix}\sqrt{\sqrt{\tilde{q}_1^2+1}-1}\\ \sqrt{\sqrt{\tilde{q}_2^2+1}-1}\\ \vdots\\ \sqrt{\sqrt{\tilde{q}_n^2+1}-1}\end{bmatrix}^T K_p \begin{bmatrix}\sqrt{\sqrt{\tilde{q}_1^2+1}-1}\\ \sqrt{\sqrt{\tilde{q}_2^2+1}-1}\\ \vdots\\ \sqrt{\sqrt{\tilde{q}_n^2+1}-1}\end{bmatrix} = -\begin{bmatrix}\sqrt{\sqrt{\tilde{q}_1^2+1}-1}\\ \sqrt{\sqrt{\tilde{q}_2^2+1}-1}\\ \vdots\\ \sqrt{\sqrt{\tilde{q}_n^2+1}-1}\end{bmatrix}^T K_p \begin{bmatrix}\frac{\tilde{q}_1}{\sqrt{\sqrt{\tilde{q}_1^2+1}-1}\sqrt{\tilde{q}_1^2+1}} & \cdots & 0\\ \vdots & \ddots & \vdots\\ 0 & \cdots & \frac{\tilde{q}_n}{\sqrt{\sqrt{\tilde{q}_n^2+1}-1}\sqrt{\tilde{q}_n^2+1}}\end{bmatrix}\dot{\boldsymbol{q}} \quad (9)$$

Because K_p is a diagonal matrix, then expression (9) is given as:

$$2\begin{bmatrix}\sqrt{\sqrt{\tilde{q}_1^2+1}-1}\\ \sqrt{\sqrt{\tilde{q}_2^2+1}-1}\\ \vdots\\ \sqrt{\sqrt{\tilde{q}_n^2+1}-1}\end{bmatrix}^T K_p \begin{bmatrix}\sqrt{\sqrt{\tilde{q}_1^2+1}-1}\\ \sqrt{\sqrt{\tilde{q}_2^2+1}-1}\\ \vdots\\ \sqrt{\sqrt{\tilde{q}_n^2+1}-1}\end{bmatrix} = -\begin{bmatrix}\frac{\tilde{q}_1}{\sqrt{\tilde{q}_1^2+1}}\\ \frac{\tilde{q}_2}{\sqrt{\tilde{q}_2^2+1}}\\ \vdots\\ \frac{\tilde{q}_n}{\sqrt{\tilde{q}_n^2+1}}\end{bmatrix}^T K_p\,\dot{\boldsymbol{q}} = -\left[\frac{\tilde{q}}{\sqrt{\tilde{q}^2+1}}\right]^T K_p\,\dot{\boldsymbol{q}} \quad (10)$$

After some algebra and using certain useful properties from the dynamics model, equation (8) can be written as:

$$\dot{V}(\tilde{\boldsymbol{q}},\dot{\boldsymbol{q}}) = \dot{\boldsymbol{q}}^{\boldsymbol{T}} M(\boldsymbol{q})\ddot{\boldsymbol{q}} + \frac{1}{2}\dot{\boldsymbol{q}}^{\boldsymbol{T}}\dot{M}(\boldsymbol{q})\dot{\boldsymbol{q}} - \left[\frac{\tilde{q}}{\sqrt{\tilde{q}^2+1}}\right]^T K_p\,\dot{\boldsymbol{q}} \quad (11)$$

$$\dot{V}(\tilde{\boldsymbol{q}},\dot{\boldsymbol{q}}) = \dot{\boldsymbol{q}}^T K_p\frac{\tilde{q}}{\sqrt{\tilde{q}^2+1}} - \dot{\boldsymbol{q}}^T K_v\frac{\dot{q}}{\sqrt{\tilde{q}^2+1}} - \dot{\boldsymbol{q}}^T B\dot{\boldsymbol{q}} - \dot{\boldsymbol{q}}^T C(\boldsymbol{q},\dot{\boldsymbol{q}})\dot{\boldsymbol{q}} + \frac{1}{2}\dot{\boldsymbol{q}}^T\dot{M}(\boldsymbol{q})\dot{\boldsymbol{q}} - \left[\frac{\tilde{q}}{\sqrt{\tilde{q}^2+1}}\right]^T K_p\,\dot{\boldsymbol{q}} \quad (12)$$

$$\dot{V}(\tilde{\boldsymbol{q}},\dot{\boldsymbol{q}}) = -\dot{\boldsymbol{q}}^T K_v\frac{\dot{q}}{\sqrt{\tilde{q}^2+1}} - \dot{\boldsymbol{q}}^T B\dot{\boldsymbol{q}} \leq 0, \quad (13)$$

The equation (13) is a globally negative semi-definite function because $K_v, B \in \mathbb{R}^{n\times n}$ are positive definite matrixes.Therefore, the stability of the equilibrium point is concluded. In order to prove global asymptotic stability, the autonomous nature of equation (6) is

exploited to apply LaSalle's invariance principle, as follows:

Let the region:

$$\Omega = \left\{ \begin{bmatrix} \tilde{\boldsymbol{q}} \\ \dot{\boldsymbol{q}} \end{bmatrix} \in \mathbb{R}^{2n} : \dot{V}(\tilde{\boldsymbol{q}}, \dot{\boldsymbol{q}}) = 0 \right\} = \{ \tilde{\boldsymbol{q}} \in \mathbb{R}^n, \dot{\boldsymbol{q}} = \boldsymbol{0} \in \mathbb{R}^n : \dot{V}(\tilde{\boldsymbol{q}}, \dot{\boldsymbol{q}}) = 0 \} \quad (14)$$

Since $\dot{V}(\tilde{\boldsymbol{q}}, \dot{\boldsymbol{q}}) \leq 0 \in \Omega$, then $V(\tilde{\boldsymbol{q}}(t), \dot{\boldsymbol{q}}(t))$is a decreasing function of t and $V(\tilde{\boldsymbol{q}}, \dot{\boldsymbol{q}})$is continuous on the compactset Ω,which is bounded from below Ω, - for example, it satisfies $V(\tilde{\boldsymbol{q}}(0), \dot{\boldsymbol{q}}(0)) \geq V(\tilde{\boldsymbol{q}}(t), \dot{\boldsymbol{q}}(t)) > 0$. Therefore, $V(\tilde{\boldsymbol{q}}(t), \dot{\boldsymbol{q}}(t))$ has a limit $\alpha \in \mathbb{R}_+$ as $t \to \infty$. Hence, $\dot{V}(\tilde{\boldsymbol{q}}(t), \dot{\boldsymbol{q}}(t)) = 0$. Since Ω is an invariant set, the unique invariant is$\tilde{\boldsymbol{q}} = \boldsymbol{0}$ and $\dot{\boldsymbol{q}} = \boldsymbol{0}$. Since the trivial solution is the unique solution of the closed-loop system (6) restrictedto Ω, then it is concluded that the origin of the state space is globally asymptotically stable.

4. Experimental setup

The experimental setup is a platform based on a three degrees-of-freedom direct-drive robot manipulator for research in robotics. It has been designed and built at the Benemérita Universidad Autónoma de Puebla, México. The robot manipulator moves in three dimensional space, as shown in Figure 2.

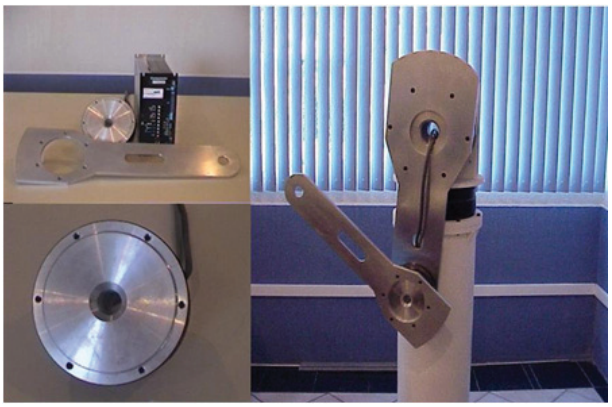

Figure 2. Experimental direct-drive robot manipulator

The experimental robot consists of links made of 6061 aluminium actuated by brushless direct-drive servo actuators from Parker Compumotor so as to drive the joints without gear reductions. The advantages of this type direct-drive servomotor include freedom from backslash and significantly lower joint friction compared with actuators composed by gear drives. The models of the servomotors used in the robot are listed in Table 1.

Link	Servomotor model	Torque [Nm]	Resolution [p/rev]
Base	DM1015A	15	4,096,000
Shoulder	DM1050A	50	4,096,000
Elbow	DM1004C	4	4,096,000

Table 1. Servomotors of the experimental robot manipulator

The servomotors are operated in torque mode and so the servos act as a torque source and accept an analogue voltage as a reference of the torque signal. Position information is obtained from incremental encoders located inside the motors. The standard backwards difference algorithm applied to the joint position measurements was used to generate the velocity signals. The workspace of the robot manipulator is a sphere with a radius of 1 m.

The electronic instrumentation is a motion control board, model MFIO3A from Precision Microdynamics Company Inc.. It is installed inside a Pentium IV computer. The MFIO3A obtains the joint position by FPGA's and the control algorithm is implemented in the language C with a sampling rate set to 2.5 ms.

With reference to the direct-drive robot manipulator, only the gravitational torque is required to implement the proposed control scheme:

$$\boldsymbol{g}(\boldsymbol{q}) = \begin{bmatrix} 0 \\ 14.28 \sin(q_2) + 1.14 \sin(q_2 + q_3) \\ 1.14 \sin(q_2 + q_3) \end{bmatrix} \quad (15)$$

5. Experimental results

This section reports an experimental comparison between a PD scheme and the proposed control on the direct-drive robot manipulator. To investigate the performance among the controllers, they have been classified as$\boldsymbol{\tau_{PD}}$for the PD control while$\boldsymbol{\tau_{src}}$represents the square root control. The experimental comparison consists in finding which provides the better performance between the evaluated controllers by using the scalar-valued$\mathcal{L}_2$ norm. A smaller $\mathcal{L}_2$ norm represents a smaller position error and, thus, the better performance.

An experiment in position control has been designed to compare the performance of$\boldsymbol{\tau_{PD}}$and $\boldsymbol{\tau_{src}}$controllers on a direct-drive robot. Extensive experiments were carried out with the two controllers. However, a representative experiment is presented. The experiment consists in moving the manipulator end-effector from its initial position to a fixed, desired position chosen as $[q_{d1}, q_{d2}, q_{d3}]^T = [45, 45, 90]^T$degrees, where q_{d1}, q_{d2}, q_{d3} represent the base, shoulder and elbow joints, respectively. The initial position and velocities were set to zero, for example in the home position.

The PD control algorithm for the experimental robot is given by:

$$\begin{matrix} \tau_{pd1} \\ \tau_{pd2} \\ \tau_{pd3} \end{matrix} = \begin{matrix} k_{p1}\tilde{q}_1 - k_{v1}\dot{q}_1 \\ k_{p2}\tilde{q}_2 - k_{v2}\dot{q}_2 + 14.28 \sin(q_2) + 1.14 \sin(q_2 + q_3) \\ k_{p3}\tilde{q}_3 - k_{v3}\dot{q}_3 + 1.14 \sin(q_2 + q_3) \end{matrix} \quad (16)$$

The three components of the square root type-control for the direct-drive arm are:

$$\begin{matrix}\tau_{sr1}\\ \tau_{sr2}\\ \tau_{sr3}\end{matrix} = \begin{matrix} k_{p1}\frac{\tilde{q}_1}{\sqrt{\tilde{q}_1^2+1}} - k_{v1}\frac{q_1^2}{\sqrt{q_1^2+1}} \\ k_{p2}\frac{\tilde{q}_2}{\sqrt{\tilde{q}_2^2+1}} - k_{v2}\frac{q_2^2}{\sqrt{q_2^2+1}} + 14.28\sin(q_2) + 1.14\sin(q_2+q_3) \\ k_{p3}\frac{\tilde{q}_3}{\sqrt{\tilde{q}_3^2+1}} - k_{v3}\frac{q_3^2}{\sqrt{q_3^2+1}} + 1.14\sin(q_2+q_3)\end{matrix} \quad (17)$$

where $\tau_{pd1}, \tau_{pd2}, \tau_{pd3}$ representthe applied torquesfor the base, shoulder and elbow joints, respectively.This is similar in form to $\tau_{sr1}, \tau_{sr2}, \tau_{sr3}$.

However, several trials for selecting the gains were necessary in order to ensure acceptable behaviour in practice - i.e., a fast response in a transitory state and a smaller steady-state error. The actual choice of the gains is, however, limited by practical considerations because it can produce saturation torque in the actuators, which deteriorates the control system performance and leads to thermal and mechanical failure. For a controller $\boldsymbol{\tau_{PD}}$,the proportional gains were chosen such that$\tau_{pdi} < |\tau_i{}^{max}|$ for $i = 1,2,3$ and $\tau_i{}^{max}$is the maximum applied torque of the *ith* joint (see the limits of the actuators in Table I). The *ith* proportional gain is given by$k_{pi} < \frac{\tau_i{}^{max}}{\tilde{q}_i(0)}$where $\tilde{q}_i(0)$ is the initial condition for the *ith* position error. The derivative gains were adjusted under the requirements to obtain put low damped response satisfying$k_{vi} \ll k_{pi}$. In the case of the controller $\boldsymbol{\tau_{src}}$, the gains were chosen as$k_{pi} < |\tau_i{}^{max}|$ for $i = 1,2,3; k_{vi} << k_{pi}$.Finally, for the given initial conditions, the proportional and derivative gains have been tuned as in Table 2.

	$\boldsymbol{\tau_{PD}}$		$\boldsymbol{\tau_{src}}$	
Link	K_p [Nm/degrees]	K_v [Nm-seg/degrees]	K_p[Nm]	K_v [Nm]
Base	k_{p1} =0.30	k_{v1} =0.12	k_{p1} =40	k_{v1} =0.8
Shoulder	k_{p2} =1.0	k_{v2} =0.45	k_{p2} =10	k_{v2} =1.5
Elbow	k_{p3} =0.04	k_{v3} =0.004	k_{p3} =0.9	k_{v3} =0.34

Table 2. Tuning up for proportional and derivative gains.

Figure 3 contains the experimental results of the position errors for the proposed controller $\boldsymbol{\tau_{src}}$corresponding to the base, shoulder and elbow joints.

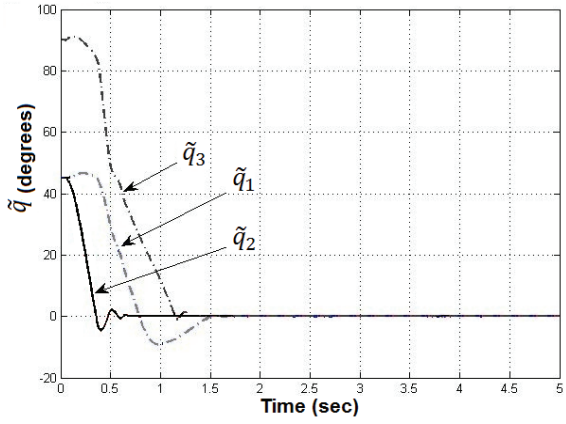

Figure 3. Experimental position errors of the proposed controller $\boldsymbol{\tau_{src}}$..

After a smooth transient ($t = 1.6\,seconds$), all the components of the position errors tend asymptotically towards a small neighbourhood convergence of zero; the steady state position errors at time t=2 s have small values of$[\tilde{q}_1(t), \tilde{q}_2(t), \tilde{q}_3(t)]^T = [0.005, 0.004, 0.006]^T$ degrees. These errors are present due to presence of static friction at the joints and a lack of static friction compensation in the control scheme.

Figure 4 contains the experimental results of the applied torque for the proposed controller $\boldsymbol{\tau_{src}}$for eachjoint. From the experimental results, these applied torques clearly evolve insidethe prescribed limits shown in Table 1.

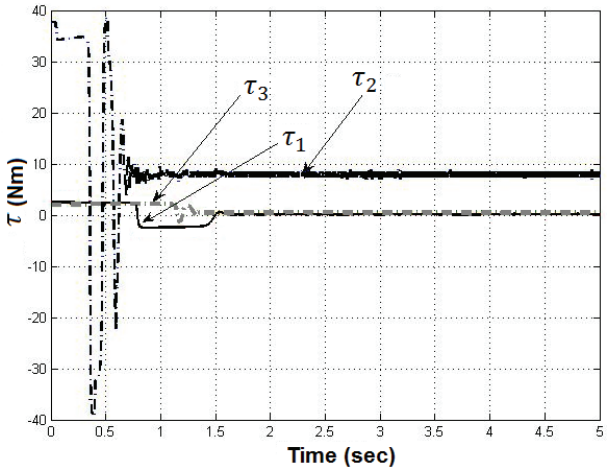

Figure 4. Applied torques of the proposed controller $\boldsymbol{\tau_{src}}$.

Figure 5 shows the experimental results of the position errors for the PD control, which evolve slowly until reaching steady state errors of $[\tilde{q}_1(t), \tilde{q}_2(t), \tilde{q}_3(t)]^T = [0.5, 0.4, 0.6]^T$ degrees. It is worth noticing that the transient state requires more time than the proposed controller. Additionally, the torque signals are inside the limits from the actuators.

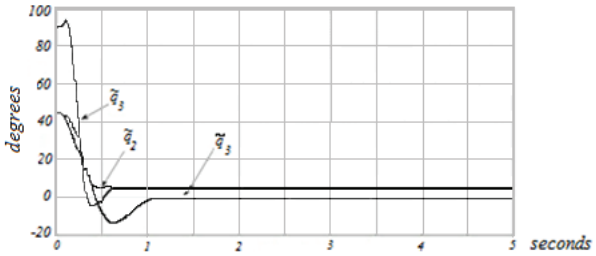

Figure 5. Experimental position errors of the PD algorithm.

The proposed controller has the property of quickly driving the position error to zero. This feature is due to its square root structure, since the position error is driven as an exponential function, the applied torque is as high as is required and this makes the control action faster, holding the actuator torque constraints thorough the saturating limits.

The $\mathcal{L}_2$ norm measures the root mean square *"average"* of the $\tilde{\boldsymbol{q}}$position error, which is:

$$\mathcal{L}_2 = \sqrt{\frac{1}{t-t_0}\int_{t_0}^{t} ||\tilde{\boldsymbol{q}}||^2 \, dt} \tag{18}$$

Where $t, t_0 \in \mathbb{R}_+$ are the initial and final times, respectively. A smaller $\mathcal{L}_2$ represents a smaller position error and, therefore, the best performance of the evaluated controller.

The main results are summarized in Figure 6, which includes the performance indexes for the $\boldsymbol{\tau_{src}}$ and $\boldsymbol{\tau_{PD}}$ controllers. For clarity, the data presented is compared with respect to the$\mathcal{L}_2$ norm of PD control. The$\mathcal{L}_2$norm for $\boldsymbol{\tau_{PD}}$ was 32 degrees and for $\boldsymbol{\tau_{src}}$ it was 12.8 degrees - the performance of the PD controller was improved, roughly, by its counterpart to the proposed controller by 60%. The proposed controller effectively exploits its square root-type exponential capacity to drive the position error to zero, having a short transient phase and a small steady-state error. Consequently, the control performance is increased in comparison with the PD scheme.

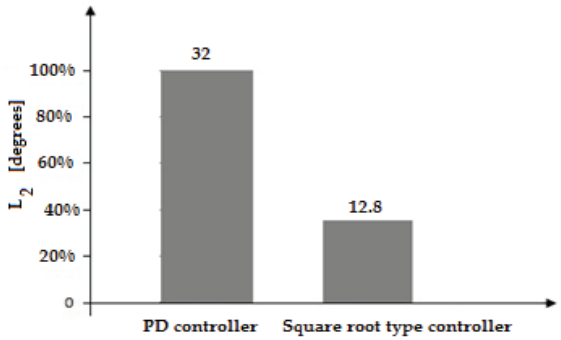

Figure 6. Indexes of performance for the evaluated controllers.

6. Conclusions

In this paper we introduced a new control scheme for the position control of robot manipulators. The proposed scheme leads to a closed-loop equilibrium point which is supported by stability analysis - in the sense of Lyapunov - and established conditions for ensuring global regulation. Such a stability proof is important in guaranteeing the suitable operation of the robotic system.

The proposed controller has a bounded smooth response such that the applied torques are inside the prescribed bounds of the servo actuator; with this controller we attempt to retain to a certain degree, the advantage of a bounded signal to overcome the saturation problems of control schemes.

For the purpose of stability, the tuning procedure for the new scheme is sufficient to select a proportional gain as diagonal positive definite matrix and a derivative gain as a positive definite matrix. The tuning up for proportional and derivative gains was chosen such that$k_{pi} < |\tau_i{}^{max}|$ for $i = 1,2,3$;and $k_{vi} << k_{pi}$.

The efficiency of the proposed scheme was corroborated through experimental tests on a real robot and good results were obtained. The performance of the proposed controller was compared with a PD control in a real-time experimental comparison on a three degrees-of-freedom direct-drive robot manipulator.

From experimental the results, the proposed scheme showed better performance, the response was smoother and without oscillations and the position error was zero due to its square root structure. Since the position error is driven as an exponential function, the applied torque is as high as is required and this makes the control action faster, holding the actuator torque constraints thorough the saturating limits. In contrast, the simple PD was observed to be less robust than the square root-type controller. The proposed controller represents an attractive scheme for the position control problem and applications in point-to-point control and pick-and-place.

7. References

[1] M. Takegaki and S. Arimoto, A new feedback method for dynamic control of manipulator, ASME J. Dynamics Syst. Measurement and Control, Vol.103, 1981,pp. 119--125.

[2] A. S. Miyazakif, Stability and robustness of PD feedback control with gravity compensation for robot manipulator, in Robotics: Theory and Application DSC, Vol.3. Edited by F. Paul, 1986.

[3] R. Kelly, Global Positioning of Robot Manipulators via PD Control Plus a Class of Nonlinear Integral Actions, IEEE Transactions on Automatic Control, Vol. 43, No. 7, 1998, pp. 934-938.

[4] R. Kelly, A tuning procedure for stable PID control of robot manipulators, Robotica Cambridge University Press, Vol. 13., 1995, pp. 141-148.

[5] J. Alvarez,V. Santibañez and R. Campa, Stability of Robot Manipulators Under Saturated PID Compensation, IEEE Transactions on Control Systems Technology, Vol. 16, No. 6, 2008, pp. 1333-1341.

[6] Y. Xu, J. M. Hollerback and D. Ma, A nonlinear PD controller for force and contact transient control, IEEE Control Systems, Vol. 15, No. 1, 1993, pp. 15-21.

[7] R. Kelly and V. Santibañez, Global Regulation of Elastic Joint Robots Based on Energy Shaping, Transactions on Automatic Control, Vol. 43, No. 10, 1998, pp. 1451-1456.

[8] V. Santibañez, R. Kelly and F. Reyes, A New Set-Point Controller with Bounded Torques for Robot Manipulators, IEEE Transactions on Industrial electronics, Vol. 45, No. 1, 1998, pp. 126-133.

[9] F. Azenc, M. Malisoff, Strict Lyapunov Function Constructions Under LaSalle Conditions With an Application to Lotka-Volterra Systems, Automatic Control, IEEE Transactions on, Vol. 55, April 2010, p.841.
[10] F. Mazenc and S. Bowong, Tracking Trajectories of Feedforward Systems, IEEE Transactions on Autumatic Control, Vol. 47, No. 8, 2002, pp.1338-1342.
[11] K. Takahashi, M. Sasaki, Remarks on tip angular position control of single-link flexible robot arm using modified Lyapunov function, International Conference on Mechatronics and Automation (ICMA), August 2010, p.1024.
[12] J. Kasac, B. Novakovic, D. Majetic and D. Brezak, Global Positioning of Robot Manipulators With Mixed Revolute and Prismatic Joints, IEEE Transactions on Automatic Control, Vol. 51,No.6, 2006, pp. 1035-1040.
[13] C. Xie and Y. Lin, A stability theorem and applications in control designs, 8th IEEE International Conference on Control and Automation (ICCA), June 2010, p.1758.
[14] V. Parra, S. Arimoto, Y. Liu, G. Hirzinger and P. Akella, Dynamic Sliding PID Control for Tracking of Robot Manipulators: Theory and Experiments, IEEE Transactions on Robotic and automation, Vol. 19, No. 6, 2003, pp. 967--976.
[15] V. Santibañez, R. Kelly and M. Llama, A novel global asymptotic stable set-point fuzzy controller with bounded torques for robot manipulators, IEEE Transactions on Fuzzy Systems, Vol. 13, No. 3,2005, pp. 362-372.
[16] H. Sun,N. Hovakimyan and B. Tamer.L1 Adaptive controller for uncertainnonlinear multi-input multi-output systems withinput quantization, IEEE Transactions onAutomatic Control, Vol. 57. No. 3, March 2012,pp. 565-578.
[17] M. W. Spongand M. Vidyasagar. Robot Dynamics and Control, John Wiley and Sons, NY, 1989.
[18] L. Sciavicco and B. Siciliano, Modeling and Control of Robot Manipulators, Springer-Verlag, London, 2005.